Environment & Ecosystem Science (EES)

DOI : http://doi.org/10.26480/ees.02.2018.30.34

ISSN: 2521-0882 (Print)
ISSN: 2521-0483 (Online)

CODEN: EESND2

PREPARATION AND CHARACTERIZATION OF $LAFEO_3$ USING DUAL-COMPLEXING AGENTS FOR PHOTODEGRADATION OF HUMIC ACID

N. Yahya[1], F. Aziz[12]*, Enriquez M.A.O[1], A. Aizat[1], J. Jaafar[1], W.J. Lau[1], N. Yusof[1], W.N.W. Salleh[1], A.F. Ismail[1]

[1] School of Chemical and Energy Engineering, Universiti Teknologi Malaysia, 81310, Skudai, Johor Bahru.
[2] Advanced Membrane Technology Research Centre, Faculty of Chemical and Energy Engineering, Universiti Teknologi Malaysia, 81310, Skudai, Johor Bahru.
Corresponding author: farhanaaziz@utm.my

ARTICLE DETAILS

Article History:

Received 10 May 2018
Accepted 6 Jun 2018
Available online 10 July 2018

ABSTRACT

Humic Acid (HA) is considered as one of the major components that represents a major fraction of dissolved in natural water. Complex mixture of organic compounds on HA lead to the problematic issue for municipal wastewater treatment plants such as undesirable taste, colour to drinking water and fouling in pipe line. The reaction of HA with chlorine during disinfection processes would produce carcinogenic by-products like trihalomethanes. In this study, for the first time, LaFeO3 photocatalyst was successfully synthesized via gel-combustion method using combined glucose/citric acid as chelating agents and was further calcined at 400°C. The photocatalytic activity of samples was investigated by degradation of Humic Acid (HA) in water under visible light irradiation. Results proved that the photocatalytic degradation of HA is dependent on the catalyst dosage, initial concentration of HA, and oxygen availability in the aeration. The photocatalytic degradation also was enhanced by high surface area of synthesized LaFeO3 obtained by amorphous structure. Overall, the percentage removal of HA by varying the catalyst dosage are in the order of 88%, 90%, 98% and 97% for 0.6 g/L, 0.8 g/L, 1.0 g/L, and 1.2 g/L respectively for an irradiation period of 120 minutes. Next, the removal of HA by manipulating its initial concentration are 98%, 90%, 85% and 86% with respect to 10 g/L, 20 g/L, 30 g/L and 40 g/L taken for 120 minutes. Overall, the optimal operational parameters for the removal of HA of catalyst dosage is 1.0 g/L performing at 98%, for initial concentration of HA which was removed efficiently at 97% is 10 g/L and via aeration in this study was about 93%, after 120 min of irradiation times.

KEYWORDS

Humic acid, gel-combustion, Lanthanum orthoferrites, adsorption, photocatalytic degradation, aeration.

1. INTRODUCTION

Humic acid, as part of natural organic matters, signifies 90% of dissolved organic carbon in surface water. It possesses extremely complex molecular structures which mainly consist of many functional groups such as carboxylic, aromatic, phenolic, hydroxide radicals, ketone and quinone groups [1]. According to numerous studies, it has been confirmed that HA could react with major disinfectants (chlorine dioxide and chlorine) to form mutagenic halogenated compounds like trihalomethanes in chlorination process of drinking water [2]. Nonetheless, it is detrimental to human health owing to its carcinogenicity. Therefore, prior to the chlorination of drinking water, it is very essential to eliminate HA. The traditional ways used to remove HA mainly contain coagulation process and ultrafiltration membranes techniques.

Advanced Oxidation Processes (AOPs) is the state of the art in the current wastewater treatment and is acknowledged as successful in eliminating complex organic contaminants due to the capability of achieving complete oxidation. AOPs have matched many advantages as compared to the conventional ways of water treatment. The process of degradation of impurities are much quicker by discharging hydroxyl radicals (•OH). The most vital variables in AOPs are catalyst and source of light to accomplish high productivity in degradation of prevailing pollutants. Despite the conventional treatments such as coagulation, membrane filtration and adsorption as the alternative of removal HA, photocatalytic oxidation has been regarded one of the latest technologies to treat various of organic contaminants [3-8]. By the generation of hydroxyl radicals (OH•) as a strong and non-selective oxidant under ambient conditions, these powerful photocatalyst can cause fast decomposition and mineralization of a wide variety of organic pollutants and natural organic matters. Recently, perovskite based-photocatalyst have been widely studied due to its visible-light-driven properties in photocatalysis [9,10]. Perovskites come under the formula ABO3 where A is an alkali rare earth like La, Ca, Sr, Ba, etc., and B is an element with valence +3 or +2, such as Fe, Cu and Ni which exhibits high proton and oxygen ion conductivity. Perovskite oxides have been of foremost importance in photocatalysis since the material exhibits a wide range of beneficial properties with low band gap, better chemical stability and environmental-friendly. One of the promising photocatalyst come from perovskites as efficient visible-light driven photocatalyst, is lanthanum orthoferrite (LaFeO3) due to its narrow band gap and optoelectronic properties [1,2,11,12].

In order to synthesize high purity of nanoparticles assisted with large surface areas and homogenous shape, numerous studies have been focused on the effect of calcination, heat treatment, solvent annealing and even concentration chelating agents [13-16]. Approach using combination of chelating agent is not being extensively study. In this study, a novel photocatalyst of LaFeO3 nanoparticles was first prepared by gel-combustion method using glucose and citric acid as combined chelating agents. The structure and morphology of the prepared LaFeO3 characterized by various analytical techniques. Then the adsorption and photocatalytic activity of LaFeO3 nanoparticles was investigated by degradation of HA in water under LED lamp under effect of effects of operational parameters such as catalyst dosage and HA initial concentration and aeration.

Photocatalytic degradation processes are controlled by oxidizing radicals,

which are photogenerated on the catalyst surface or in the bulk solution. Hydroxyl radicals, •OH, with their high oxidizing potential, and eventually peroxide radicals, O2−•, that enhance •OH radical formation in water, are the most interesting species in organic pollutant photocatalytic degradation 8. Consequently, the application of a dosage method that avoids high pollutant concentrations to control the photo-oxidation reaction offers a plausible alternative. Thus, the highest degradable concentration will be progressively added, according to the surface-active center concentration, so that catalyst saturation or poisoning and the formation of non-photoactive intermediates that hamper the target pollutant degradation, are avoided or reduced. Largely, main purpose of aeration is used for accelerating the mixing of suspension photocatalyst in the case of slurry reactors and economical source of oxygen 2. Recently, aeration is applied as one of a determining parameter for promoting the adsorption and photocatalytic performance because it acts as an oxygen supply for the reaction 11. The photocatalytic degradation can be triggered due to the formation of more oxygen active species in the HA. The results indicated that sufficient amount of
oxygen as electron acceptor and oxidizing agents in aeration significantly gives impact on adsorption and photocatalytic degradation.

2. EXPERIMENTAL

2.1 Synthesizing LaFeO3 nanoparticle using gel-combustion method

Lanthanum (III) Nitrate Hexahydrate, La(NO3)3.6H2O and glucose were purchased from Merck Co Ltd. Ferum (III) Nitrate Nonahydrate, Fe(NO3)3.9H2O, citric acid and ammonia hydroxide are purchased from Sigma-Aldrich Ltd. For targeted pollutant, Humic acid (HA) was employed to test the photocatalytic activity under visible light irradiance using LED (100 W) light source (Phoenix Electric Co., Ltd. Himeji Japan). All reagents were analytical grade and used without further purification. Firstly, sequence of appropriate amount of Lanthanum Nitrate Hexahydrate (La(NO3)3.6H20), Iron (III) Nitrate Nonahydrate (Fe(NO3)3.9H2O) and citric acid monohydrate (C6H8O7.H2O) were added into distilled water. Ratio between (C6H8O7.H2O) and metal nitrate were fixed as 2:1. The mixture was stirred while heated at 70 °C. While the mixture was still stirred with magnetic stirrer, 80% glucose solution was added into the beaker. The pH was then controlled at 7 by added NH4OH. The temperature of stirred-solution was increased up to 200 °C until xerogel was formed. The xerogel was then heated in an oven at 250 °C until the xerogel became black powder, so-called "as-burnt powder". The as-burnt powder was calcined at 400 °C for 2 h.

2.2 Characterization of synthesized LaFeO3

The crystallinity of sample was examined using XRD (Rigaku Smartlab D/MAX 2500) with Cu (k=1.5406 Å) irradiation and scanned in the range of 20˚- 90˚ at a rate of scanning of 1˚C/min, particle morphologies and composition of samples were evaluated using FESEM (Supra 35-VP, Carl Zeiss, Germany) and SEM-EDX (Hitachi TM 3000 Tabletop Microscope). The surface areas were measured and calculated using BET method based on nitrogen gas adsorption-desorption (Micromeritics Instrument Corporation TriStarII 3020 (surface area and porosity analyzer).

2.3 Photocatalytic degradation of humic acid

The photocatalytic degradation activity of Humic acid by LaFeO3 was carried out in customized photo reactor. The visible light irradiation, placed 10 cm from the specimen, was sourced from LED light (100W). 0.18 g, 0.24 g, 0.30 g and 0.36 g of synthesized LaFeO3 was weighed and dispersed in 300 ml of HA (10mg/L) respectively. Prior to degradation, LaFeO3 was allowed to reach adsorption-desorption equilibrium for at least 30 minutes under continuous stirring, followed by irradiation of visible light for 120 minutes. To observe the effects of initial concentration on photocatalytic activity, the initial concentration was varied at 10 mg/L, 20 mg/L, 30 mg/L, and 40 mg/L respectively. The effects of aeration were carried by continuously aerated the solution by a pump to provide oxygen during photocatalytic test. At specific time intervals, 5 mL aliquot was taken using filtered syringe to separate LaFeO3. Concentration of HA were monitored by measuring the value of absorbance of aliquot using UV-Vis spectrophotometer at λ= 254nm. The performance of adsorption and photocatalysis were further calculated and evaluated by using the following equation (Equation 1):

$$\text{Removal of HA (\%)} = \frac{C_0 - C_t}{C_0} \times 100\% \quad (1)$$

Where Co (mg/L) is the initial concentration of HA, Ct (mg/L) is the concentration at time interval.

3. RESULTS AND DISCUSSION

3.1 Characterization results of synthesized LaFeO3

Figure 1 shows XRD diagram of the synthesized samples with glucose/citric acid calcined at 400◦C for 2 h. As shown at Figure 1, no crystalline phase was observed which corresponded to the amorphous powder. The crystallinity of nanoparticles mostly no formed at range of 300◦C -400◦C due to the transformation of nanoparticle into crystallinity form by the loss of water and organics from prepared materials. Since there is very limited of mobility of the ions at that temperature, it could take some time to improve crystallinity to a great extent. However, previous study stated that the amorphous structure exhibited better photocatalytic performance than crystalline structure [17]. It was revealed that amorphous products displayed high surface area when comparing to other crystalline products that could lead to high adsorption of pollutants on surface of photocatalyst [18]. Defect condition on amorphous surface also could enhance the absorption of light and help to lower the recombination of photogenerated electrons and holes, which further improve the photocatalytic degradation performance [18]. The BET surface area of the synthesized LaFeO3 with glucose/citric acid was found to be highest (70 m2 g−1) compared to previous synthetized LaFeO3 70 m2 g−. High surface area of photocatalyst is vital for the removal of any pollutants because it can provide more active site for the reaction to be complete within a short time [19].

As shown in Figure 2, FESEM micrograph images of the LaFeO3 particles provide the information about morphology of the synthesized samples. Despite their amorphous phase (Figure 1), the morphology incredibly showed uniform spherical shape-like and composed of homogenous, less agglomerated particles which contrary to most of previous study related to morphology of amorphous nanoparticles [20].

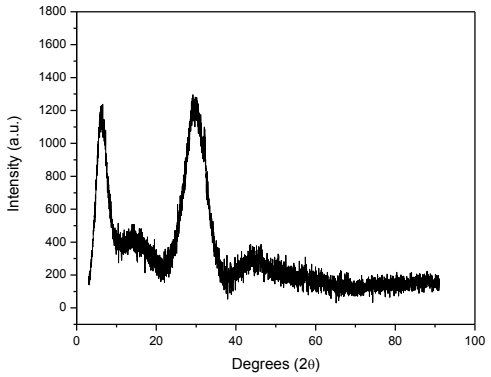

Figure 1: XRD pattern of the LaFeO3 powder sample with glucose/citric acid calcined at 400°C for 2 h.

The EDX analysis was employed to determine the element of the synthesized material. As shown in the Figure 3(a), EDX mapping suggests that La (blue), Fe (light blue) and O (red) elements are distributed uniformly in the samples. Based on the EDX analysis Figure 3(a), the elements present are La, Fe and O with a mole ratio of 1:1:3 corresponding to the stoichiometric composition of LaFeO3. The composition of the elements in the sample obtained by the glucose/citric acid gel combustion method was 71.38%; 14.10%; and 14.52% for Oxygen; iron and oxygen, respectively (Table 1).

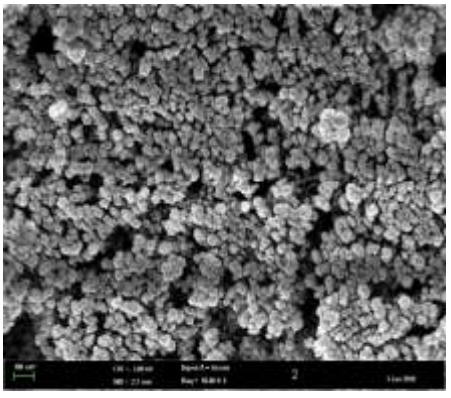

Figure 2: FESEM images of the LaFeO3 powder sample with glucose/citric acid calcined at 400 °C for 2 h.

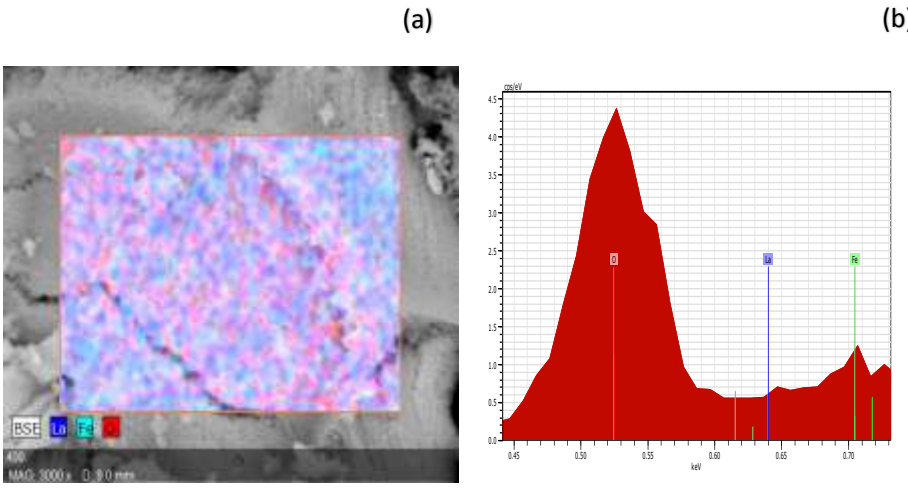

Figure 3: (a) Elemental mapping of LaFeO3 (b) EDX analysis of the calcined LaFeO3 with glucose/citric acid callcined at 400 °C for 2 h

Table 1: The chemical composition of the BiFeO3.

Elements	La	Fe	O
Analytical percentage (%)	71.38%;	14.10%	14.52%

3.2 Effect of catalyst dosage

In order to study the effects of catalyst dosage, 0.18 g, 0.24 g, 0.30 g and 0.36 g of synthesized LaFeO3 were weighed and dispersed in 300 mL of HA (10mg/L). The results of the experimental studies are depicted in Figure 4. As seen in the figure, the degradation efficiency increased with the increasing catalyst dosage from 0.6 g/L to 1.0 g/L; thereafter, at the catalyst dosage of 1.2 g/L, the degradation efficiency decreased. At lower maximum catalyst dosages, low active sites were available, while at higher maximum catalyst dosages, agglomerated particles, high turbidity, and scattering effects might cause lower degradation efficiency. Results indicate that low initial LaFeO3 dosage (0.6 g/L) degradation is very slow. Only 88% HA removal is achieved, and the catalyst experience slow photocatalytic degradation after 30 minutes of adsorption. This may be explained by considering that the elevated organic concentration on the catalyst surface yields the formation of non-photoactive adsorbed intermediates which are progressively accumulated and are probably contaminating the catalyst surface. As a result, the degradation becomes slower [21]. Moreover, HA removal results from Figure 4 shows that with 1.0 g/L dosage, achieved 98% and is considered the optimum dosage for this parameter. Consequently, dosage increases HA degradation efficiently and it occurs only up to 1.0 g/L and then decreases at 1.2 g/L dosage. A cleaner catalyst surface, lower probabilities for active centres blockage and formation of non-photoactive intermediates may explain these results. Nonetheless, according to Dona et.al, the catalyst surface features are very important as they determine the reaction mechanism. In contrast, at low concentrations, the catalyst surface features and molecule-surface interactions affect degradation rate at lower extent, being mainly determined by the production of OH• radicals.

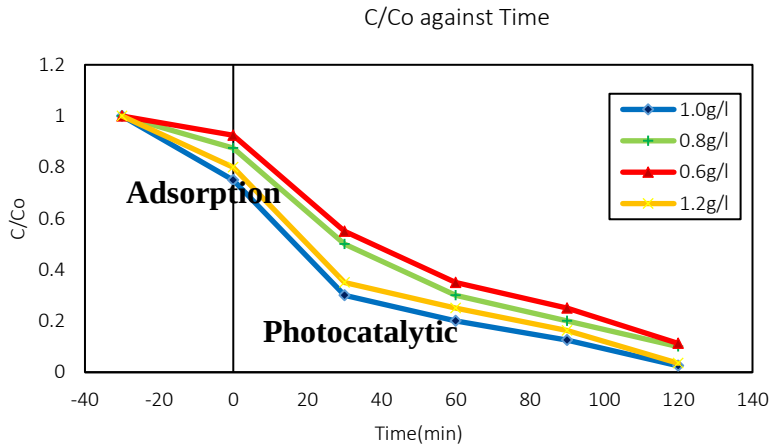

Figure 4: Effect of catalyst on LaFeO3 of adsorption and photocatalytic degradation HA (pH = 6, HA = 10 mg/L, contact time = 120 minutes).

3.3. Effect of initial concentration of HA

To study the effects of initial concentration, 10 g/L, 20 g/L, 30 g/L and 40 g/L of HA were prepared beforehand. The results of the experimental studies are depicted in Figure 5. It was observed that, photocatalytic activity performance achieved removal in the order of 98%, 90%, 85% and 86% for 10 g/L, 20 g/L, 30 g/L and 40 g/L respectively after irradiated by visible light within 120 minutes. The results presented in Figure 5 show that the lower initial concentration of HA exhibited the best photocatalytic performance. Conferring to Saleh et. al., at higher initial concentrations of HA, the penetration of light that could travel to the active site of the catalyst was blocked, resulting in a decrease in the total number of active sites that played roles in the degradation process. As investigated by Nezamzadeh-Ejhieh et. al., it has been reported that photocatalytic activity depends on the number of active species that play important roles in the photocatalytic process. During irradiation, excited electrons in the conduction band of the catalyst react with the oxygen molecules (O2) to form superoxide radicals (•O2). In contrast, holes left behind in the valence band of the catalyst will react with water (H2O) or hydroxyl (OH–) molecules to form hydroxyl radicals (•OH). These active radicals are known as strong reducers and oxidizers, which can destroy the complex chemical bonds of contaminants such as HA. The lowest degradation was obtained 30 g/L, indicating that the total number of active sites had decreased for the photodegradation of HA.

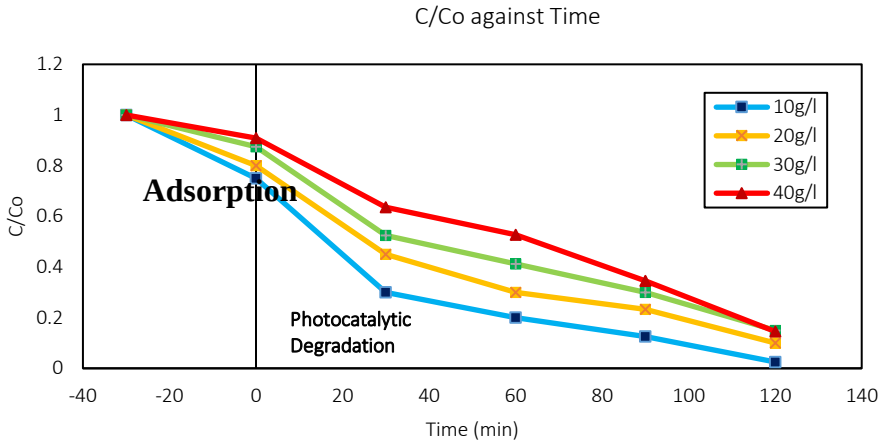

Figure 5: Effect of initial concentration on LaFeO3 of adsorption and photocatalytic degradation HA (pH = 6, HA = 10 mg/L, Catalyst dosage = 0.1-gram, contact time = 120 minutes).

3.4 Effect of aeration

In order to study the effects of aeration, series of performance test involving stirring (without aeration) and with aeration were carried out. The results of the experimental studies are depicted in Figure. 6. It was observed that with aeration, the removal of HA via adsorption was 22%. Contrary in the case of no aeration, the adsorption removal was only 14%. The adsorption performance was induced by presence of aeration in this study compared with no aeration. However, in the case of aeration, the photocatalyst surface may become highly hydroxylated to the point of inhibiting the adsorption of HA and thus slows down the reaction rate [22]. For the photocatalytic activity performance with aeration, it is observed the removal efficiency of HA increased from 22% to 43% after irradiated by visible light and achieved 93% removal within 120 minutes. Compared with no aeration, removal efficiency of HA increased only from 18% to 32% after irradiated by visible light and only achieved 88% removal within 120 minutes.

Similar results were observed, which stated that photocatalytic performance was triggered by the excess amount of oxygen in aeration [23]. The presence of oxygen enhanced photocatalytic degradation since it will react with conduction band electrons to form superoxide radial anions which eventually yield reactive •OH [24]. The oxygen supplied into the HA could prevent the recombination between electron and hole which would reduce the photocatalytic activity. As the LaFeO3 irradiated by visible light, an electron is excited out of its energy level to conduction band and leaves a positive hole in the valence band. The positive hole is a strong oxidant which can either react with electron donors like OH- or H2O to form •OH or oxidized the HA directly. The excited electron can be trapped by oxygen molecules from air bubbling to form •O2 on the surface of LaFeO3. Henceforth, the photocatalytic degradation can be triggered due to the formation of more oxygen active species in the HA. It was reported that the usage of air enhanced the degradation as compared to pure oxygen demonstrating that oxygen is required only at minimum concentration [25]. With aeration, numerous bubbles are made and will cause scatter light before arriving at the photocatalytic surface during reaction. Compared with no aeration, the initial dissolved oxygen is fatigued, and a large percent of excited electrons should recombine with positive holes and get back to the valence state [8]. Henceforth, the photocatalytic degradation in aeration samples can be enhanced due to the formation of more oxygen active species in the wastewater [26-29].

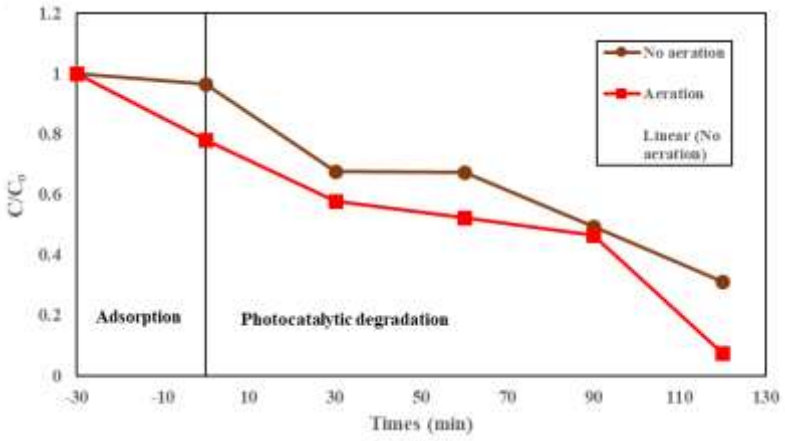

Figure 6: Effect of aeration on LaFeO3 of adsorption and photocatalytic degradation HA (pH = 6, HA = 10 mg/L, Catalyst dosage = 0.1 gram, contact time = 120 minutes, air flow rate of 0.62 L. min-1. kg-1).

4. CONCLUSION

In this study, potential photocatalyst, LaFeO3 is synthesized via gel-combustion using dual-complexing agents, glucose and citric acid and further calcined at 400˚C. The photocatalyst is tested on removal of HA via adsorption and photocatalytic degradation. Due to existence of amorphous structure of LaFeO3, high surface area is obtained. The high surface area of synthesized LaFeO3 promote adsorption and photocatalytic performance within 120 minutes. The results also indicated that the adsorption and degradation of HA is dependent on the catalyst dosage, initial concentration of HA and oxygen availability in the aeration. The presence of oxygen as electron acceptor in the aeration samples prevent from recombination of electron-holes thus enhance the photocatalytic degradation. Overall, the optimal operational parameters for the removal of HA of catalyst dosage is 1.0 g/L performing at 98%, for initial concentration of HA which was removed efficiently at 97% is 10 g/L and via aeration in this study was about 93%, after 120 min of irradiation times. Therefore, synthesized LaFeO3 can be used as a promising photocatalyst to be applied for the removal of Humic Acid in municipal wastewater treatment in future.

ACKNOWLEDGEMENT

I am very grateful to my patience yet zealous supervisor, Dr. Farhana Binti Aziz who had shown her earnest support as a mentor through all the discussions and motivations towards the accomplishment to complete my final year project. I would like to articulate my thankfulness to Ms. Syazwani Binti Yahya for assisting and guiding me to bring this project into success.

REFERENCES

[1] Peng, K., Fu, L., Yang, H., Ouyang, J. 2016. Perovskite LaFeO3/montmorillonite nanocomposites: synthesis, interface characteristics and enhanced photocatalytic activity. Scientific Reports, 6, 19723. doi:10.1038/srep19723 http://www.nature.com/articles/srep19723#supplementary-information

[2] Thirumalairajan, S., Girija, K., Ganesh, I., Mangalaraj, D., Viswanathan, C., Balamurugan, A., Ponpandian, N. 2012. Controlled synthesis of perovskite LaFeO3 microsphere composed of nanoparticles via self-assembly process and their associated photocatalytic activity. Chemical Engineering Journal, 209, 420-428. doi:http://dx.doi.org/10.1016/j.cej.2012.08.012

[3] Loganathan, K., Saththasivam, J., Sarp, S. 2018. Removal of microalgae from seawater using chitosan-alum/ferric chloride dual coagulations. Desalination, 433, 25-32. doi:https://doi.org/10.1016/j.desal.2018.01.012

[4] Choi, H., Stathatos, E., Dionysiou, D.D. 2006. Sol–gel preparation of mesoporous photocatalytic TiO 2 films and TiO 2/Al 2 O 3 composite membranes for environmental applications. Applied Catalysis B: Environmental, 63 (1), 60-67

[5] Basha, S., Keane, D., Morrissey, A., Nolan, K., Oelgemöller, M., Tobin, J. 2010. Studies on the Adsorption and Kinetics of Photodegradation of Pharmaceutical Compound, Indomethacin Using Novel Photocatalytic Adsorbents (IPCAs). Industrial & Engineering Chemistry Research, 49 (22), 11302-11309. doi:10.1021/ie101304a

[6] Abdullah, N.S.A., So'aib, S., Krishnan, J. 2017. Effect of calcination temperature on ZnO/TiO2 composite in photocatalytic treatment of phenol under visible light. Malaysian Journal of Analytical Sciences, 21 (1), 173-181.

[7] Kanakaraju, D., Ahmad, N.L.B., Sedik, N.B.M., Long, S.G.H., Guan, T.M., Chin, L.Y. 2017. Performance Of Solar Photocatalysis And Photo-Fenton Degradation Of Palm Oil Mill Effluent. Malaysian Journal of Analytical Sciences, 21 (5), 996-1007.

[8] Mekprasart, W., Pecharapa, W. 2011. Synthesis and characterization of nitrogen-doped TiO2 and its photocatalytic activity enhancement under visible light. Energy Procedia, 9, 509-514.

[9] Mera, A.C., Váldes, H., Jamett, F.J., Meléndrez, M.F. 2017. BiOBr microspheres for photocatalytic degradation of an anionic dye. Solid State Sciences, 65, 15-21. doi:https://doi.org/10.1016/j.solidstatesciences.2017.01.001

[10] Qin, C., Li, Z., Chen, G., Zhao, Y., Lin, T. 2015. Fabrication and visible-light photocatalytic behavior of perovskite praseodymium ferrite porous nanotubes. Journal of Power Sources, 285, 178-184. doi:http://dx.doi.org/10.1016/j.jpowsour.2015.03.096

[11] Mutalib, M.A., Aziz, F., Jamaludin, N.A., Yahya, N., Ismail, A.F., Mohamed, M.A., Yusof, N. 2018. Enhancement in photocatalytic degradation of methylene blue by LaFeO3-GO integrated photocatalyst-adsorbents under visible light irradiation. Korean Journal of Chemical Engineering, 35 (2), 548-556. doi:10.1007/s11814-017-0281-0

[12] Patrick, R., Aziz, F., Yahya, N., Jamaludin, N., Ismail, N. 2017. Preparation and Characterization of TiO2-LaFeO3 based Mixed Matrix Membrane for Oily Wastewater Treatment. Journal of Applied Membrane Science and Technology, 20 (1).

[13] Wang, Y.W., Yuan, P.H., Fan, C.M., Wang, Y., Ding, G.Y., Wang, Y.F. 2012. Preparation of zinc titanate nanoparticles and their photocatalytic behaviors in the photodegradation of humic acid in water. Ceramics International, 38 (5), 4173-4180.

[14] Wang, D.G., Ming, X.C., Zhang, W.L., Zhang, J.H., Chen, C.Z. 2018. Effect of heat treatment on the properties of HA/BG composite films. Ceramics International, 44 (6), 7228-7233. doi:https://doi.org/10.1016/j.ceramint.2018.01.173

[15] Aziz, F., Ismail, A., Aziz, M., Soga, T. 2014. Effect of solvent annealing on the crystallinity of spray coated ternary blend films prepared using low boiling point solvents. Chemical Engineering and Processing: Process Intensification, 79, 48-55.

[16] Tahir, M.B., Nabi, G., Khalid, N.R., Rafique, M. 2018. Role of europium on WO3 performance under visible-light for photocatalytic activity. Ceramics International, 44 (5), 5705-5709. doi:https://doi.org/10.1016/j.ceramint.2017.12.223

[17] Xie, J., Yang, C., Duan, M., Tang, J., Wang, Y., Wang, H., Courtois, J. 2018. Amorphous NiP as cocatalyst for photocatalytic water splitting. Ceramics International, 44 (5), 5459-5465. doi:https://doi.org/10.1016/j.ceramint.2017.12.179

[18] Wang, Y., Li, L., Zhang, Y., Zhang, N., Fang, S., Li, G. 2017. Crystalline-to-amorphous transformation of tantalum-containing oxides for a superior performance in unassisted photocatalytic water splitting. International Journal of Hydrogen Energy, 42 (33), 21006-21015. doi:https://doi.org/10.1016/j.ijhydene.2017.07.064

[19] Huang, D., Miyamoto, Y., Ding, J., Gu, J., Zhu, S., Liu, Q., Zhang, D. 2011. A new method to prepare high-surface-area N–TiO 2/activated carbon. Materials letters, 65 (2), 326-328.

[20] Shen, H., Xue, T., Wang, Y., Cao, G., Lu, Y., Fang, G. 2016. Photocatalytic property of perovskite LaFeO3 synthesized by sol-gel process and vacuum microwave calcination. Materials Research Bulletin, 84, 15-24. doi:https://doi.org/10.1016/j.materresbull.2016.07.024

[21] Doña, J.M., Araña, C.G.J., Pérez, J., Colón, G., Macías, M., Navio, J.A. 2015. The effect of dosage on the photocatalytic degradation of organic pollutants. Res.Chem.Intermed., 33 (3-5), 351-358.

[22] Kim, J.K., Jang, D.G., Campos, L.C., Jung, Y.W., Kim, J.H., Joo, JC. 2016. Synergistic removal of humic acid in water by coupling adsorption and photocatalytic degradation using TiO2/coconut shell powder composite. Journal of Nanomaterials, 28.

[23] Adishkumar, S., Kanmani, S., Rajesh Banu, J. 2014. Solar photocatalytic treatment of phenolic wastewaters: influence of chlorides, sulphates, aeration, liquid volume and solar light intensity. Desalination and Water Treatment, 52 (40-42), 7957-7963.

[24] Rauf, M., Meetani, M., Hisaindee, S. 2011. An overview on the photocatalytic degradation of azo dyes in the presence of TiO2 doped with selective transition metals. Desalination, 276 (1-3), 13-27.

[25] Huston, P.L., Pignatello, J.J. 1999. Degradation of selected pesticide active ingredients and commercial formulations in water by the photo-assisted Fenton reaction. Water Research, 33 (5), 1238-1246.

[26] Lee, S.L., Ho, L.N., Ong, S.A., Wong, Y.S., Voon, C.H., Khalik, W.F., Nordin, N. 2018. Role of dissolved oxygen on the degradation mechanism of Reactive Green 19 and electricity generation in photocatalytic fuel cell. Chemosphere, 194, 675-681. doi:https://doi.org/10.1016/j.chemosphere.2017.11.166

[27] Nezamzadeh-Ejhieh, A., Ghanbari-Mobarakeh, Z. 2015 J. Ind. Eng. Chem., 21, 668

[28] Saleh, R., Djaja, N.F. 2014 Superlattice. Microst. 74 217

[29] Wang, W., Tade, M.O., Shao, Z. 2015. Research progress of perovskite materials in photocatalysis- and photovoltaics-related energy conversion and environmental treatment. Chemical Society Reviews, 44 (15), 5371-5408. doi:10.1039/C5CS00113G ronment & Ecosystem Science , 2(2) : 25-29.